Aeroelasticity in Turbomachines

Fernando Sisto

Abstract Turbomachines also prone to various types of dynamic instabilities and responses that in some respects are similar to those of classical aeroelasticity as described in earlier chapters. However the complications of rotating flows and structures provide new challenges as described in this chapter, also see the related discussion in chapters "Modeling of Fluid-Structure Interaction and Modern Analysis for Complex" and "Nonlinear Unsteady Flows in Turbomachinery".

The advent of the jet engine and the high performance axial-flow compressor toward the end of World War II focussed attention on certain aeroelastic problems in turbomachines.

The concern for very light weight in the aircraft propulsion application, and the desire to achieve the highest possible isentropic efficiency by minimizing parasitic losses led inevitably to axial-flow compressors with cantilever airfoils of high respect ratio. Very early in their development history these machines were found to experience severe vibration of the rotor blades at part speed operation; diagnosis revealed that these were in fact stall flutter (see chapter "Stall Flutter") oscillations. The seriousness of the problem was underlined by the fact that the engine operating regime was more precisely termed the 'part corrected speed' condition, and that in addition to passing through this regime at ground start up, the regime could be reentered during high flight speed conditions at low altitude. In either flight condition destructive behavior of the turbojet engine could not be tolerated.

In retrospect it is probable that flutter had occurred previously in some axial flow compressors of more robust construction and in the later stages of low pressure axial-flow stream turbines as well. Subsequently a variety of significant forced and self-excited vibration phenomena have been detected and studied in axial-flow turbomachinery blades.

In 1987 and 1988 two volumes of the AGARD *Manual on Aeroelasticity in Turbomachines* [1, 2] were published with 22 chapters in all. The sometimes disparate topics contributed by nineteen different authors and/or co-authors form a detailed and extensive reference base related to the subject material of the present chapter.

F. Sisto (✉)
Mechanical Engineering, Stevens Institute of Technology, Hoboken, NJ, USA

E. H. Dowell (ed.), *A Modern Course in Aeroelasticity*, Solid Mechanics and Its Applications 264, https://doi.org/10.1007/978-3-030-74236-2_8

The reader is urged to refer to the AGARD compendium for in-depth development and discussion of many of the topics to be introduced here, and for related topics (such as the role of experimentation) not included here.

1 Aeroelastic Environment in Turbomachines

Consider an airfoil or blade in an axial flow turbine or compressor which is running at some constant rotational speed. For reasons of steady aerodynamic and structural performance the blade has certain geometric properties defined by its length, root and tip fixation, possible mechanical attachment to other blades and by the chord, camber, thickness, stagger and profile shape which are functions of the radial coordinate. Furthermore, the blade may be constructed in such a manner that the line of centroids and the line of shear centers are neither radial nor straight, but are defined by schedules of axial and tangential coordinates as functions of radius. In fact, in certain cases, it may not be possible to define the elastic axis (i.e., the line of shear centers). The possibility of a built-up sheet metal and spar construction, a laid-up plastic laminate construction, movable or articulated fixations and/or supplemental damping devices attached to the blade would complicate the picture even further.

The blade under consideration, which may now be assumed to be completely defined from a geometrical and kinematical point of view, is capable of deforming[1] in an infinite variety of ways depending upon the loading to which it is subjected. In general, the elastic axis (if such can be defined) will assume some position given by axial and tangential coordinates which will be continuous functions of the radius (flapwise and chordwise bending). About this axis a certain schedule of twisting deformations may occur (defined, say by the angular displacement of a straight line between leading and trailing edges). Finally, a schedule of plate type bending deformations may occur as functions of radius and the chordwise coordinate. (Radial extensions summoned by centrifugal forces may further complicate the situation).

Although divergence is not a significant problem in turbomachines, an alternative static aeroelastic problem, possibly resulting in the measurable untwist and uncamber of the blades, can have important consequences with respect to the steady performance and with respect to the occurrence of blade stall and surge.

One has now to distinguish between steady and oscillatory phenomena. If the flow through the machine is completely steady in time and there are no mechanical disturbances affecting the blade through its connections to other parts of the machine, the blade will assume some deformed position as described above (and as compared to its manufactured shape) which is also steady in time. This shape or position will depend on the elastic and structural properties of the blade and upon the steady aerodynamic and centrifugal loading. (The centrifugal contribution naturally does not apply to a stator vane.)

[1] Deformations are reckoned relative to a steadily rotating coordinate system in the case of a rotor blade.

Consider the situation, however, where dynamic disturbances may exist in the airstream, or may be transmitted through mechanical attachments from other parts o the structure. Due to the unsteadiness of the aerodynamic and/or the external forces the blade will assume a series of time-dependent positions. If there is a certain repetitive nature with time of the displacements relative to the equilibrium position, the blade is said to be executing vibrations, the term being taken to include those cases where the amplitude of the time-dependent displacements is either increasing, decreasing or remaining constant as time progresses.

It is the prediction and control of these vibrations with which the turbomachine aeroelastician is concerned. Once the blade is vibrating the aerodynamic forces are no longer a function only of the airstream characteristics and the blade's angular position and velocity in the disturbance field, but depend in general upon the blade's vibratory position, velocity and acceleration as well. There is a strong interaction between the blade's time-dependent motion and the time-dependent aerodynamic forces which it experiences. It is appropriate at this point to note that in certain cases the disturbances may be exceedingly small, serving only to 'trigger' the unsteady motion, and that the vibration may be sustained or amplified purely by the interdependence or feedback between the harmonic variation with time of the blade's position and the harmonic variation with time of the aerodynamic forces (the flutter condition).

A further complication is that a blade cannot be considered as an isolated structure. There exist aerodynamic and possibly structural coupling between neighboring blades which dictate a modal description of the entire vibrating bladed-disk assembly. Thus an interblade phase angle, σ, is defined and found to play a crucial role in turbomachine aeroelasticity . Nonuniformities among nominally 'identical' blades in a row, or stage, are found to be extremely important in turbomachine aeroelasticity; stemming from manufacturing and assembly tolerances every blade row is 'mistuned' to a certain extent, i.e., the nominally identical blades in fact are not identical.

2 The Compressor Performance Map

The axial flow compressor, and its aeroelastic problems, are typical; the other major important turbomachine variant being the axial flow turbine (gas or steam). In the compressor the angle of attack of each rotor airfoil at each radius r is compounded of the tangential velocity of the airfoil section due to rotor rotation and the through flow velocity as modified in direction by the upstream stator row. Denoting the axial component by V_x and the angular velocity by Ω as in Fig. 1, it is clear that the angle of attack will increase inversely with the ratio $\phi = V_x/(r\Omega)$. In the compressor, an increase in angle of attack (or an increase in 'loading') results in more work being done on the fluid and a greater stagnation pressure increment Δp_0 being imparted to it. Hence the general aspects of the single 'stage' (i.e., pair of fixed and moving blade rows) characteristics in Fig. 2 are not without rational explanation. Note that

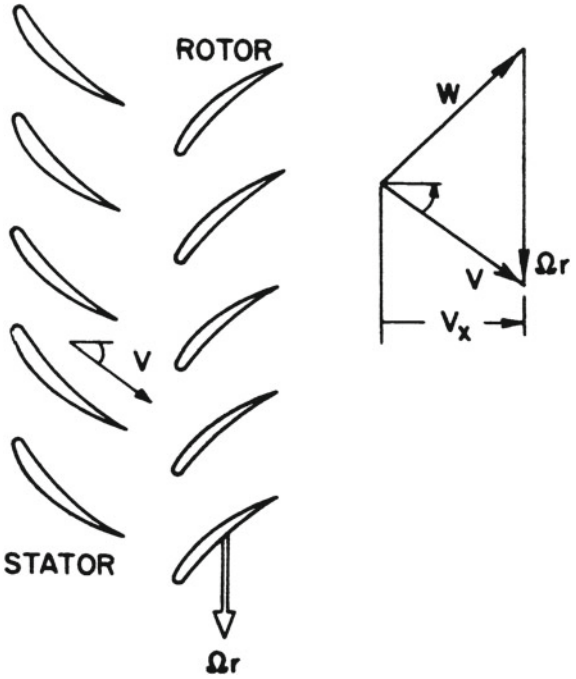

Fig. 1 Velocity triangle in an axial compressor

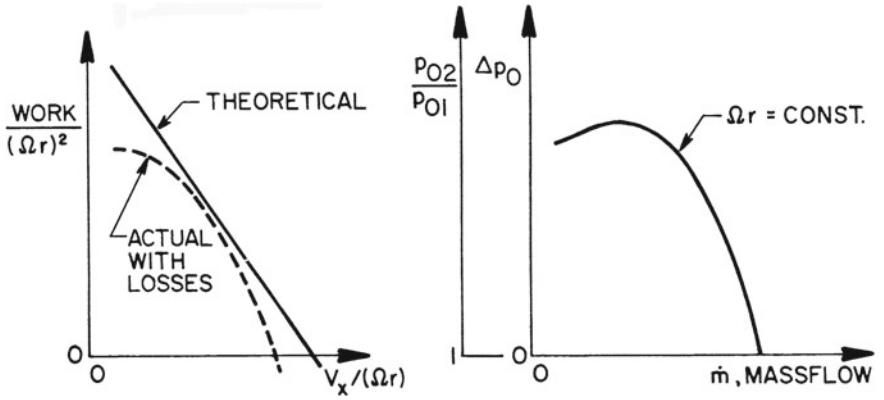

Fig. 2 Work and pressure ratio relationships

the massflow through the stage equals the integral over the flow annulus of the product of V_x and fluid density.

When the various parameters are expressed in dimensionless terms, and the complete multistage compressor is compounded of a number of states, the overall compressor 'map', or graphical representation of multistage characteristics, appears as in

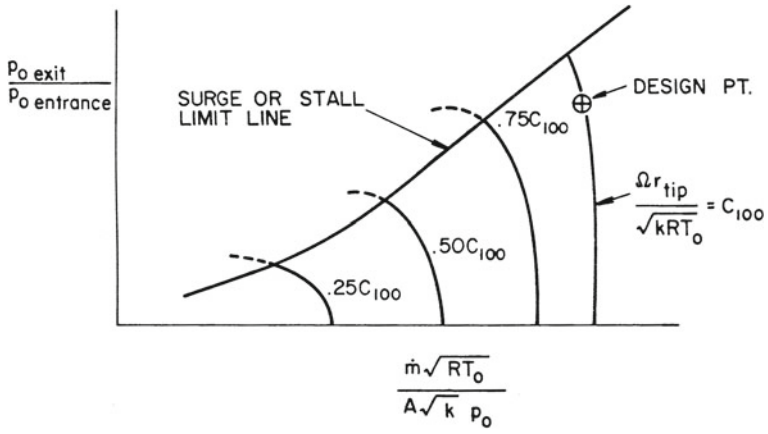

Fig. 3 Compressor map

Fig. 3, where $\dot{m}$ is massflow, γ and R are the ratio of specified heats and gas constant, respectively; T_0 is stagnation temperature and A is a reference flow area in the compressor. Conventionally the constants γ and R are omitted where the identity of the working fluid is understood (e.g., air). The quantity A is a scaling parameter relating the absolute massflow of geometrically similar machines and is also conventionally omitted. The tangential velocity of the rotor blade tip, Ωr_{tip}, is conventionally replaced by the rotational speed in rpm. The latter omission and replacement are justified when discussing a particular compressor.

An important property of the compressor map is the fact that to each point there corresponds theoretically a unique value for angle of attack (or incidence) at any reference airfoil section in the compressor. For example, taking a station near the tip of the first rotor blade as a reference, contours of incidence may be superposed on the map coordinates. In Fig. 4 such angle contours have been shown for a specific machine. As defined here, a_i is the angle between the relative approach velocity W and the chord of the airfoil. Here again axial velocity V_x (or massflow) is seen to display an inverse variation with respect to angle of attack as a line of constant rotational speed is traversed. The basic reason such incidence contours can be established is that the two parameters which locate a point on the map, $\dot{m}\sqrt{T_0/p_0}$ and $\Omega r/\sqrt{T_0}$, are effectively a Mach number in the latter case and a unique function of Mach number in the former case. Thus the 'Mach number triangles' are established which yield the same 'angle of attack' as the velocity triangles to which they are similar, Fig. 5.

As a matter for later reference, contours of $V/(v\omega)$ for a particular stator airfoil, or else $W/(b\omega)$ for a particular rotor airfoil, can be superimposed on the same map, provided the environmental stagnation temperature, T_0, is specified. These contours are roughly parallel, though not exactly, to the constant rotational speed lines. The natural frequency of vibration, ω, tends to be constant for a rotor blade at a given rotational speed; and of course a stator blade's frequency does not depend directly on rotation. However, upon viewing the velocity triangles in Fig. 5, it is clear that if Ωr

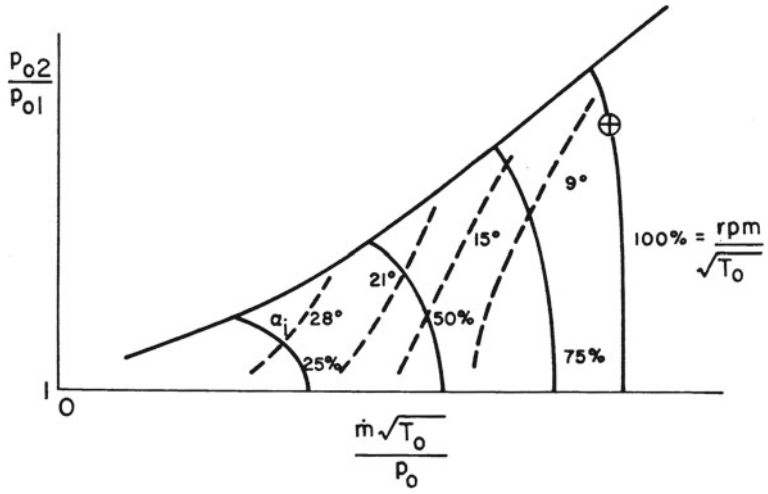

Fig. 4 Map showing incidence as a parameter

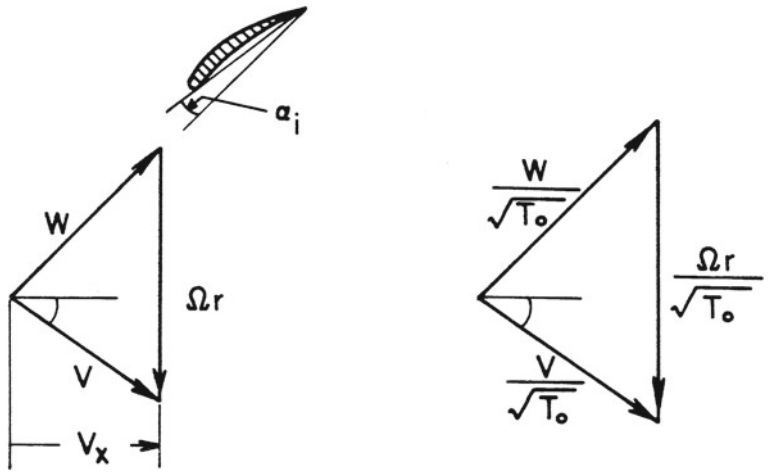

Fig. 5 Velocity and Mach number correspondence

is kept constant and the *direction* of V is kept constant, the size of W may increase or decrease as V_x (or massflow) is changed. In fact, if the angle between V and W is initially close to 90 degrees, a not uncommon situation, the change in the magnitude of W will be minimal. For computing the stator parameter, $V/(b\omega)$, the direction of W *leaving* a rotor is considered to be virtually constant, and the corresponding changes in V (length and direction) as V_x is varied lead to similar conclusions with regard to angle of attack and magnitude of V experienced y the following stator. The values of $W/(b\omega)$ increase with increasing value of Ωr_{tip}, since the changes in W

(or V) will dominate the somewhat smaller changes in the appropriate frequency ω, at least in the first few stages of the compressor. Compressibility phenomena, when they become significant will sometimes alter these general conclusions.

3 Blade Mode Shapes and Materials of Construction

Flutter and vibration of turbomachinery blades can and do occur with a wide variety of these beam -like structures and their degrees of end restraint. Rotor blades in use vary from cantilever with perfect root fixity all the way to a single pinned attachment such that the blade behaves in bending like a pendulum 'flying out' and being maintained in a more or less radial orientation by the centrifugal (rather than a gravity) field. Stator vanes may be cantilevered from the outer housing or may be attached at both ends, with degrees of fixity ranging from 'encastred' to 'pinned'.

The natural modes and frequencies of these blades, or blade -disc systems when the blades are attached to their neighbors in the same row or the discs are not effectively rigid, are obtainable by standard methods of structural dynamics. Usually twisting and two directions of bending are incorporated in a beam -type finite element analysis. If plate-type deformations are significant, the beam representation must be replaced by more sophisticated plate or shell elements which recognize static twist and variable thickness.

In predicting the first several natural modes and frequencies of rotor blades it is essential to take into account the effect of rotor rotational speed. Although the description is not analytically precise in all respects, the effect of rotational speed can be approximately described by stating $\omega_n^2 = \omega_{0n}^2 + K_n\Omega^2$ where ω_{0n} is the static (nonrotating) frequency of the rotor blade and the Southwell coefficient K_n is a proportionality constant for any particular blade in the nth mode. The effect is most pronounced in the natural modes which exhibit predominantly bending displacements; the modes associated with the two gravest frequencies are usually of this type, and it is here that the effect is most important. A positive Southwell coefficient represents a centrifugal stiffening of the blade, increasing the natural frequency. Disk rotation rate also produces a softening effect that can reduce the Southwell coefficient. This softening effect is typically significant for only the first mode. High temperatures in high pressure turbines operating at high power levels can reduce the modulus of elasticity of the blades, reducing the static natural frequency ω_{0n}. As high engine power tends to occur at high rotor speeds, thermal effects can cause the frequency of some blade modes to decrease with increasing speed. Other factors also need to be considered, such as blade fixity boundary condition (fixed-fixed in stators versus fixed-free in rotors), and disk flexibility.

Materials of construction are conventionally aluminum alloys, steel or stainless steel (high nickel and/or chromium content). However, in recent applications titanium and later beryllium have become significant. In all these examples, considering flutter or forced vibration in air as the surrounding fluid, the fluid/structural mass ratios are such that the critical mode and frequency may be taken to be one or a combination of the modes calculated, or measured, in a vacuum.

More recently there has been a reconsideration of using blades and vanes made of laminated materials such as glass cloth, graphite or metal oxide fibers laid up in polymeric or metal matrix materials and molded under pressure to final airfoil contours. Determining the modes and frequencies of these composite beams is more exacting. However, once determined, these data may be used in the same manner as with conventional metal blades. It should also be noted that aeroelastic programs related to turbomachinery often make a great deal of practical use out of mode and frequency data determined experimentally from prototype and development hardware.

A major consideration in all material and mode of construction studies is the determination of mechanical damping characteristics. Briefly stated the damping may be categorized as material or structural. The former is taken to describe a volume-distributed property in which the rate of energy dissipation into heat (and thus removed from the mechanical system) is locally proportional to a small power of the amplitude of the local cyclical strain. The proportionality constant is determined by many factors, including the type of material, state of mean or steady strain, temperature and other minor determinants.

The structural damping will usually be related to interfacial effects, for example in the blade attachment to the disk or drum, and will depend on normal pressure across the interface, coefficient of friction between the surfaces, mode shape of vibration, and modification of these determinants by previous fretting or wear. Detailed knowledge about damping is usually not known with precision, and damping information is usually determined and used in 'lumped' or averaged fashion. Comparative calculations may be use to predict such gross damping parameters for a new configuration, basing the prediction on the known information for an existing and somewhat similar configuration. By this statement it is not meant to imply that this is a satisfactory state of affairs. More precise damping prediction capabilities would be very welcome in modern aeroelastic studies of turbomachines, and some studies of this nature are reported in Refs. [1, 2].

The aeroelastic response is central to the analysis of fatigue and fracture of turbomachinery blades. The question of crack initiation, crack propagation and destructive failure cannot be addressed without due attention being given to the type of excitation (forced or self-excited) and the parametric dependencies on the nonsteady aerodynamic forces. This may be appreciated when it is noted that the modal shape functions, frequencies and structural damping of a blade change with the crack growth of the specimen. This concatenation of aeroelasticity and blade failure prediction is presently an active area of research and development.

4 Nonsteady Potential Flow in Cascades

Unwrapping an annulus of differential height dr from the blade row flow passage of an axial turbomachine results in a two-dimensional representation of a cascade of airfoils and the flow about them. The airfoils are identical in shape, equally spaced, mutually congruent and infinite in number.

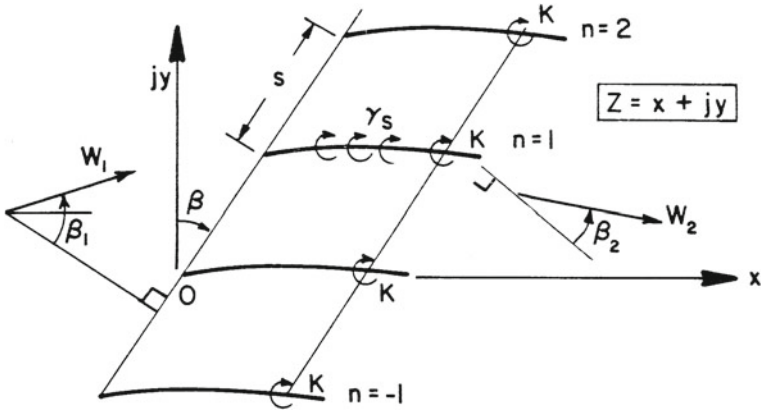

Fig. 6 Cascade camberlines modelled by vortex sheets

When a cascade is considered, as opposed to a single airfoil, the fact that the flexible blades may be vibrating means that the relative pitch and stagger may be functions of time and also position in the cascade. The steady flow, instead of being a uniform stream, will now undergo turning; large velocity gradients may occur in the vicinity of the blades and in the passages between them. These complications imply that the blade thickness and steady lift distribution must be taken into account for more complete fidelity in formulating the nonsteady aerodynamic reactions. See chapters by Whitehead and Verdon in Ref. [1].

A fundamental complication which occurs is the necessity for treating the wakes of shed vorticity from *all* the blades in the cascade.

Assume the flow is incompressible. Standard methods of analyzing steady cascade performance provide the steady vorticity distribution common to all the blades, $\gamma_s(x)$, and its dependence on W_1 and β_1. As a simple example of cascading effects consider only this steady lift distribution on each blade in the cascade and compute the disturbance velocity produced at the reference blade by a vibration of al the blades in the cascade.

In what follows the imaginary index j for geometry and the imaginary index i for time variation (i.e., complex exponential) cannot be 'mixed'. That is $ij \neq -1$. Furthermore, it is convenient to replace the coordinate normal to the chord, z, by y and the upwash on the reference airfoil w_a by v. The velocities induced by an infinite column of vortices of equal strength, τ, are given by (Fig. 6)

$$\delta[u(z) - jv(z)] = \frac{j\Gamma}{2\pi} \sum_{n=-\infty}^{\infty} \frac{1}{Z - \zeta_n} \tag{4.1}$$

where the location ζ_n of the nth vortex

$$\zeta_n = \xi + jnse^{-j\beta} + jY_n(\xi_n, t) + X_n(t) \tag{4.2}$$

indicates small deviations from uniform spacing s, ($Y_n \ll s$, $X_n \ll c$). The point Z is on the zeroth or reference blade

$$Z = x + jY(x, t) + X(t) \tag{4.3}$$

and the location of the vortices will ultimately be congruent points on different blades so that

$$\xi_n = \xi + ns \sin\beta \tag{4.4}$$

(The subscript naught, indicating the zeroth blade, is conventionally omitted.) Finally, harmonic time dependence with time lag $-r$ between the motions of adjacent blades[2] is indicated by

$$Y_n(\xi_n, t) = e^{in\omega r}\, Y(\xi, t) \tag{4.5}$$

With these provisions the Cauchy kernel in (4.1) may be written

$$\frac{1}{Z - \zeta_n} = \frac{1}{x - \xi - jnse^{-j\beta} + j[Y(x, t) - Y_n(\xi_n, t)] + X(t) - X_n(t)} \tag{4.6}$$

and summing (4.5) over all blades

$$\sum_{n=-\infty}^{n=\infty} \frac{1}{Z - \zeta_n} = \frac{1}{x - \xi + j[Y(x, t) - Y(\xi, t)]} + \sum_{n=-\infty}^{\infty'} \frac{1}{Z - \zeta_n} \tag{4.7}$$

where the primed summation indicates $n = 0$ is excluded. The first term on the RHS of (4.7) is a self-induced effect of the zeroth foil. The part $Y(x, t) - Y(\xi, t)$ is conventionally ignored in the thin-airfoil theory; it is small compared to $x - \xi$ and vanishes with $x - \xi$. Hence the first term supplies the single airfoil or self-induced part of the steady state solution. Expanding the remaining term yields

$$\begin{aligned} \sum{}' \frac{1}{Z - \zeta_n} \cong \sum{}' \frac{1}{x - \xi - jns\, e^{-j\beta}} + j \sum{}' \frac{Y_n(\xi_n,\, t) - Y(x,\, t)}{(x - \xi - jns\, e^{-j\beta})^2} \\ + \sum{}' \frac{X_n(t) - X(t)}{(x - \xi - jns\, e^{-j\beta})^2} + \cdots \end{aligned} \tag{4.8}$$

[2] This so-called 'periodicity assumption' of unsteady cascade aerodynamics lends order, in principle and often in practice, to the processes of cascade aeroelasticity. The mode of every blade is assumed to be identical, with the same amplitude and frequency but with the indicated blade-to-blade phase shift. Such a blade row, would be termed 'perfectly tuned'. Absent this assumption, the cascade representing a rotor of n blades could have n distinct components (type of mode, modal amplitude, frequency).

where the last two summations on the RHS of (4.8) are the *time-dependent portions*. The corresponding unsteady induced velocities from (4.1) may be expressed as follows using the preceding results

$$\delta[\tilde{u}(x')-j\tilde{v}(x')] \simeq -\frac{\gamma_s(\xi')\delta\xi'}{2\pi c}\mathbf{P}^2\Big\{\sum{}' \frac{e^{in\omega\tau}Y(\xi',\ t)-Y(x',\ t)}{(\chi-jn\pi)^2} + \frac{1}{j}\sum{}' \frac{e^{in\omega\tau}X(t)-X(t)}{(\chi-jn\pi)^2}\Big\} \tag{4.9}$$

where the primed variables are dimensionless w.r.t. the chord,

$$P = \pi e^{j\beta}c/s \tag{4.10}$$

$$\chi = P(x'-\xi') \tag{4.11}$$

and $\tilde{u}$, $\tilde{v}$ are the time dependent parts of u, v. The local chordwise distribute vortex strength $\gamma_s(\xi)d\xi$ has replaced τ the discrete vortex strength in the last step, (4.9). With the notation

$$q = 1-\omega\tau/\pi \tag{4.12}$$

the summations may be established in closed form. For example, when the blades move perpendicular to their chordlines with the same amplitude all along the chord (pure bending) the displacement function is a constant

$$Y = -\bar{h}e^{i\omega t} = -h \tag{4.13}$$

and, upon integrating over the chord in (4.9), one obtains

$$\tilde{u}(x') - j\tilde{v}(x') = \frac{\mathbf{P}^2}{2\pi c}\int^{1_0\gamma_s}(\xi')\sum{}' \frac{e^{in\omega\tau}h(t)-h(t)}{(\chi-jn\pi)^2}d\xi' \tag{4.14}$$

or

$$\tilde{u} = -\frac{h}{2\pi c}\int_0^1 \gamma_s(\xi')[F-iI]d\xi' \tag{4.15a}$$

$$\tilde{v} = -\frac{h}{2\pi c}\int_0^1 \gamma_s(\xi')[G+iH]d\xi' \tag{4.15b}$$

where

$$F+iG = \mathbf{P}^2\frac{q\sinh\chi\ \sinh q\chi-\cosh\chi\ \cosh q\chi+1}{\sin h^2\chi} \tag{4.15c}$$

$$H+iI = \mathbf{P}^2\frac{q\sinh\chi\ \cosh q\chi-\cosh\chi\ \sinh q\chi}{\sin \mathrm{h}^2\chi} \tag{4.15d}$$

Similar disturbance velocity fields can be derived for torsional motion, pure chordwise motion, etc. Another separate set of disturbance fields may be generated to take account of the blade thickness effects by augmenting the steady vorticity distribution $\gamma(x)$ by, say $-j\epsilon(x)$, the steady source distribution, in the above development.

The net input to the computation of oscillatory aerodynamic coefficients is then obtained by adding the $\tilde{v}$ of all the effects so described to the LHS of the integral equation which follows

$$\overbrace{v_1(x)+v_2(x)+v_3(x)}^{\text{on } y=0,\ 0<x<c} = \frac{1}{2\pi}\int_0^c [\gamma_1(\xi)+\gamma_2(\xi)+\gamma_3(\xi)]K(\xi-x)d\xi + \frac{1}{2\pi}\int_c^\infty [\gamma_1(\xi)+\gamma_2(\xi)+\gamma_3(\xi)]K(\xi-x)d\xi \tag{4.16}$$

In this formulation v_1 may be identified with the unsteady upwash, if any, convected as a gust with the mean flow and v_2 is the unsteady upwash attributable to vibratory displacement of all the blades in the cascade, where each blade is represented by steady vortex and source/sink distribution. It is v_2 that was described for one special component (pure bending) in the derivation of $\tilde{v}$ leading to (4.15b).

The component v_3 may be identified with the unsteady upwash elative to the zeroth airfoil occasioned by its harmonic vibration.

Since we are dealing here with a linear problem each of the subscripted subproblems may be solved separately and independently of the others. It is also important to note that since the vortex distributions γ_1, γ_2 and γ_3 representing the lift distributions on the cascade chordlines are unsteady they must give rise to distributions of free vortices in the wake of each airfoil of the cascade. In other words vortex wakes emanate from the trailing edge of each airfoil and are convected downstream: at a point with fixed coordinates in the wake, the strength of the vortex element instantaneously occupying that point will vary with time. Hence, the integral equation will in general contain a term that is an integral over the wake ($c < \xi < \infty$) to account for the additional induced velocities from the infinite number of semi-infinite vortex wakes. The kernel $\frac{1}{2}\pi K(\xi - x)$ accounts in every case for the velocity induced at $(x, 0)$ by a vortex element at the point $(\pi, 0)$ on the chord or wake of the reference, or zeroth, airfoil plus an element of equal strength located at the congruent point $(\pi + ns\sin\beta, ns\cos\beta)$ of every other profile of the cascade or its wake. The form of K may in fact be derived by returning to the previous derivation for $\tilde{v}$ in (4.9) and (4.15b) and extracting the terms

$$\overbrace{\frac{1}{\xi-x}}^{\text{isolated airfoil}} + \overbrace{\sum_{n=-\infty}^{\infty}\frac{1}{\xi-x+jns\,e^{-j\beta}}}^{\text{cascade effect}} \tag{4.17}$$

In this expression the signs have been changed to imply calculations of positive v (rather than $-jv$) and with each term it is now necessary to associate a strength

$\gamma_r(\xi)\exp(in\omega r)$ ($r = 1, 2$ or 3) since the inducing vortexes now pulsate rather than being steady in time. The kernel now appears as

$$\frac{1}{2\pi}K(\xi - x) = \frac{1}{2\pi}\sum_{n=-\infty}^{\infty}\frac{e^{in\omega\tau}}{\xi - x + jns\exp(-j\beta)} \tag{4.18}$$

which may be summed in closed form to yield

$$\frac{1}{2\pi}K(\xi - x) = \frac{e^{j\beta}}{2s} \cdot \frac{\cosh[(1-\sigma/\pi)\pi\exp(j\beta)(\xi - x)/s] + ij\,\sinh[(1-\sigma/\pi)\pi\,\exp(j\beta)(\xi - x)/s]}{\sinh[\pi\exp(j\beta)(\xi - x)/s]} \tag{4.19}$$

where $\sigma = \omega\tau$ is known as the interblade phase angle, an assumed constant.

The term for $n = 0$ in the summation (4.18) is

$$\frac{1}{2\pi}K_0(\xi - x) = \frac{1}{2\pi}\frac{1}{\xi - x} \tag{4.20}$$

which is the kernel for the isolated airfoil. Hence, the added complexity of solving the cascaded airfoil problem is attributed to the additional terms giving the more complicated kernel displayed in (4.19).

In contradistinction to the isolated airfoil case, solutions of the unsteady aerodynamics integral equation cannot be solved in closed form, or in terms of tabulated functions, for arbitrary geometry (β and s/c) and arbitrary interblade phase angle, σ. In fact, as noted previously, the thickness distribution of the profiles and the steady lift distribution become important when cascades of small space/chord ratio are considered to vibrate with nonzero interblade phasing. Consequently, solutions to the equation are always obtained numerically. It is found that the new parameters β, s/c and σ are strong determinants of the unsteady aerodynamic reactions. A tabular comparison of the effect of these variables on the lift due to bending taken from the data in [3] appears below. In this chart, the central stencil gives the *lift coefficient* for the reference values of $s/c = 1.0$, $\beta = 45°$, $\sigma = 0.4pi$. Other values in the matrix give the coefficient resulting from changing one and only one of the governing parameters.

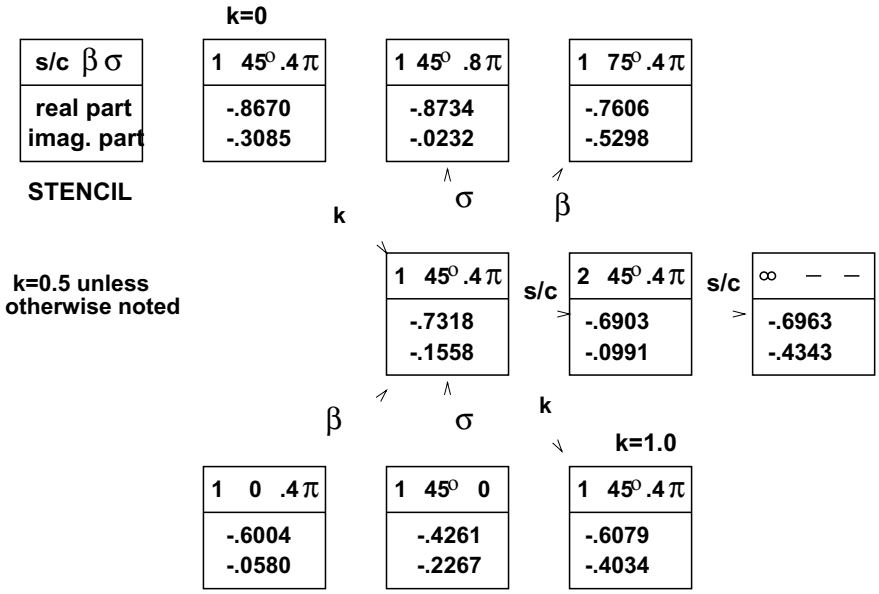

The effects of thickness and steady lift cannot be easily displayed, and are conventionally determined numerically for each application. See Chap. III in [1].

5 Compressible Flow

The linearized problem of unsteady cascade flow in a compressible fluid may be conveniently formulated in terms of the acceleration potential, $-p/\rho$, where p is the perturbation pressure, i.e., the small unsteady component of fluid pressure. Using the acceleration potential as the primary dependent variable, a number of compact solutions have been obtained for the flat plate cascade at zero incidence. The most reliable in subsonic flow is that due to Smith [4], and in supersonic flow the solutions of Verdon [5] and Adamczyk [6] are representative.

Supersonic flow relative to the blades of a turbomachine is of practical importance in steam turbines and near the tips of transonic compressor blades. In these cases the axial component of the velocity remains subsonic; hence analytic solutions in this flow regime (the so-called subsonic leading edge locus) are of the most interest. It may be that in future applications the axial component will be supersonic. In this event the theory actually becomes simper so that the present concentration on subsonic values of M_{axial} represents the most difficult problem. Currently efforts are underway to account for such complicating effects as changing back-pressure on the stage, flow turning, shock waves, etc.

To illustrate the effect of varying the Mach number from incompressible on up to supersonic, a particular unsteady aerodynamic coefficient has been graphed in Fig. 7 as a function of the relative Mach number. It is seen that the variation of the coefficient

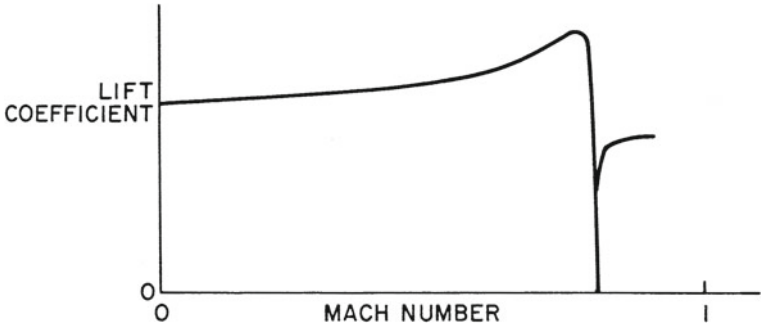

Fig. 7 The aerodynamic resonance phenomenon

in the subsonic regime is not great except in the immediate neighborhood of the so-called 'resonant' Mach number, or the Mach number at which 'aerodynamic resonance' occurs.

It is possible to generalize the situation with respect to compressibility by indicating that the small disturbance approximations are retained, but the velocities, velocity potential, acceleration potential, or pressure (in every case the disturbance component of these quantities) no longer satisfy the Laplace equation, but rather an equation of the following type.

$$(1 - M^2)\phi_{xx} + \phi_{yy} = \frac{1}{a^2}\phi_{tt} - 2\frac{M}{a}\phi_{xt} = 0 \tag{5.1}$$

Here M is the relative Mach number and a is the sound speed. Note that the presence of time derivatives make this partial differential equation hyperbolic whatever the magnitude of M, a situation quite different from the steady flow equation.

Although the above equation is appropriate to either subsonic or supersonic flow, the resonance phenomenon occurs in the regime of subsonic axial component of the relative velocity when geometric and flow conditions satisfy a certain relationship.

Equating the time of propagation of a disturbance along the cascade to the time for an integral number of oscillations to take place plus the time lag associated with the interblade phase angle, σ, yields

$$\frac{s}{V_p^+} = \frac{2\pi v}{\omega} - \frac{\sigma}{\omega} \tag{5.2a}$$

$$\frac{s}{V_p^-} = \frac{2\pi v}{\omega} + \frac{\sigma}{\omega} \tag{5.2b}$$

where $V_p^{\pm}$, the velocity of propagation, has two distinct values associated with the two directions along the cascade, see Fig. 8.

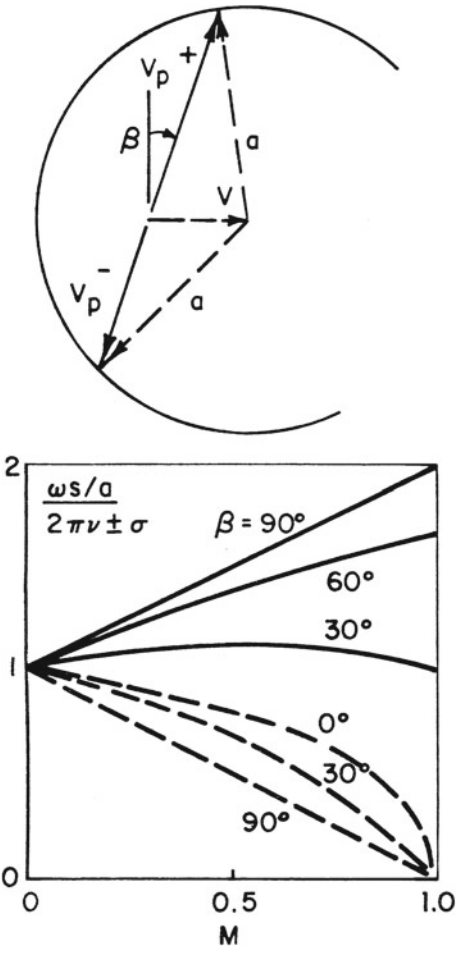

Fig. 8 Resonant values of governing parameters

$$V_p^{\pm} = a[\sqrt{1 - M^2 \cos^2 \beta} \pm M \sin \beta] \tag{5.3}$$

These expressions can be reduced to the equation

$$\frac{\omega s}{a} = (2\upsilon\pi \pm \sigma)(\sqrt{1 - M^2 \cos^2 \beta} \mp M \sin \beta) \tag{5.4}$$

where υ may be any positive integer, and with the upper set of signs may also be zero.

Equation (5.4) may be graphed and potential acoustic resonances discerned by plotting the characteristics of a given stage on the same sheet for possible coincidence. (It is convenient to take β as the parameter with axes $\omega s/a$ and M.) Acoustic resonances of the variety described above may be dangerous because they account for

the vanishing, or near vanishing, of all nonsteady aerodynamic reactions including therefore the important aerodynamic damping. Although it is difficult to establish with certainty, several cases of large vibratory stresses have been correlated with the onset of acoustic resonance. It should be recognized that the effects of blade thickness and nonconstant Mach number throughout the field are such as to render the foregoing formulation somewhat approximate.

The foregoing development may also be based more rigorously on the theoretically derived integral equation relating the harmonically varying downwash on the blade to the resulting harmonically varying pressure difference across the blade's thickness. Symbolically

$$\bar{v}_a(x) = \int_0^c K(\xi - x)\Delta\bar{p}_a(\xi)d\xi \tag{5.5}$$

and the acoustic resonance manifests itself by a singularity appearing in the kernel K for special values of k, s, c, τ and β of which K is a function. Under this circumstance the downwash υ_a can only remain finite, as it must physically, by a vanishing of Δp_a as noted above. The previous development shows why the compressible flow solutions have received such an impetus from, and are so closely related to, the acoustic properties of compressor and fan cascades.

Thus the field of aeroacoustics, as exemplified in the text of Goldstein [7], and the field of turbomachine aeroelasticity are in a synergistic relationship. This is discussed more fully in [1].

The acoustic resonance phenomenon, as just described results from standing waves in blade-fixed coordinates, albeit with impressed throughflow velocity, of the fluid occupying the interblade passages.

6 Periodically Stalled Flow in Turbomachines

Rotating, or propagating, stall are terms which describe a phenomenon of circumferentially asymmetric flow in axial compressors. Such a flow usually appears at rotationally part-speed conditions and manifests itself as one or more regions of reduced (or even reversed) throughflow which rotate about the compressor axis at a speed somewhat less than rotor speed, albeit in the same direction.

A major distinction between propagating stall and surge is that in the former case the integrated massflow over the entire annulus remains steady with time whereas in the latter case this is not true. The absolute propagation rate can be brought to zero or even made slightly negative by choosing pathological compressor design parameters.

If the instigation of this phenomenon can be attributed to a single blade row (as it obviously must in a single-stage compressor) then insofar as this blade row is concerned, it represents a periodic stall ing and unstall ing of each blade in the row. Later or preceding blade rows (i.e., half-stage) may or may not experience individual

blade stall periodically, depending on the magnitude of the flow fluctuation at that stage, as well as the cascade stall limits in that stage.

The regions of stall ed flow may extend across the flow annulus (full span) or may be confined either to the root or tip regions of the blades (partial-span stall) The number of such regions which may exist in the annulus at any one time varies from perhaps 1 to 10 with greater numbers possible in special types of apparatus.

The periodic loading and unloading of the blades may prove to be extremely harmful if a resonant condition of vibration obtains. Unfortunately the frequency of excitation cannot be accurately predicted at the present time so that avoidance of resonance is extremely difficult.

The results of various theories concerning propagating stall are all moderately successful in predicting the propagational speed. However the number of stall patches which occur (i.e., the circumferential wavelength of the disturbance) seems to be analytically unpredictable so that the frequency of excitation remains uncertain. Furthermore, the identification of the particular stage which is controlling the propagating stall , in the sense noted above, is often uncertain or impossible.

This situation with regard to propagating stall has recently been impacted by a CFD approach using the vortex method of description. In chapter "Stall Flutter" the vortex method was applied to the analysis of stall flutter. The earlier application, however, was to propagating (or rotating) stall, i.e. for the flow instability which can occur with completely rigid blades. The vortex method has been intensively developed for propagating stall prediction and results [9] indicate that success in the long sought objective of wavelength prediction is at hand. Improvements that are required for more useful results are in the boundary layer subroutine executed at each time step for each blade) and in the enlargement of computing capacity to handle the number of blades in realistic annular cascades. A further improvement that is desirable is in the vortex merging algorithm. The vortex method is a time-marching CFD routine in which the location of a large number of individual vortices are tracked on the computational domain. New vortices are created at each time step to satisfy the boundary conditions and separation criteria. Hence, to limit the total number of vortices in the field after many time steps, it is necessary to merge individual vortices, preferably downstream of the cascade. Many merging criteria may be considered, related to the strength and position of the candidate vortices.

Although the precise classification of vibratory phenomena of an aeromechanical nature is often somewhat difficult in turbomachines because of the complication due to cascading and multistaging, it is nevertheless necessary to make such distinctions as are implied by an attempt at classification. The manifestation of stall flutter in turbomachines is a good example of what is meant. When a given blade row, or cascade, approaches the install ing incidence in some sense (i.e., stall ing defined by rapid increase of relative total pressure loss, or defined by rapid increase in deviation angle, or defined by the appearance of flow separation from the suction surface of the blades, etc.) it is found experimentally that a variety of phenomena may exist. Thus the region of reduced throughflow may partially coalesce into discrete patches which propagate relative to the cascade giving rise to the type of flow instability previously discussed under rotating stall. There is no dependence on blade flexibility.

Under certain other overall operating conditions it is found that in the absence of, or even coexistent with, the previous manifestation, the blades vibrate somewhat sporadically at or near their individual natural frequencies. There is no immediately obvious correlation between the motions of adjacent blades, and the amplitudes of vibrations change with time in an apparently random manner. (We exclude here all vibration attributable to resonance with the propagating stall frequency, should the propagation phenomenon also be present.) This behavior is termed stall flutter or stall ing flutter and the motion is often in the fundamental bending mode. Another term is random vibration. Since the phenomenon may be explained on the basis of nonlinear mechanics, (see the chapter on Stall Flutter) the sporadicity of the vibration can be attributed provisionally to the fact that the excitation has not been strong enough to cause 'entrainment of frequency', a characteristic of many nonlinear systems. Hence, each blade vibrates, *on the average*, as if the adjacent blades were not also vibrating. However, a careful analysis demonstrates that the instantaneous amplitude of a particular blade is effected somewhat by the 'instantaneous phase difference' between its motion and the motion of the adjacent blade(s). One must also speak of 'instantaneous' frequency since a frequency modulation is also apparent. As a general statement it must be said that the frequency, amplitude and phase of adjacent blades are functionally linked in some complicated aeromechanical manner which results in modulations of all three qualities as functions of time. While the frequency modulation will normally be small (perhaps less than 1 or 2%) the amplitude and the phase modulations can be quite large. Here the term phase difference has been used rather loosely to describe the relationship between two motions of slightly different frequency. Since this aerodynamic coupling would also depend on the instantaneous amplitude of the adjacent blade(s), it is not surprising that the vibration gives a certain appearance of randomness. On the linear theory for identically tuned blades one would not expect to find sporadic behavior as described above. However, it is just precisely the failure to satisfy these two conditions that accounts for the observed motion; the average blade system consists of an assembly of slightly detuned blades (nonidentical frequencies) and furthermore the oscillation mechanism is nonlinear.

Application of vortex method aerodynamics to a cascade of elastically supported blades recently has demonstrated [12], in a computational sense, the features of randomness and sporadicity as described above.

When the relative magnitudes of the nonsteady aerodynamic forces increase it may be expected that entrainment of frequency will occur. In certain nonlinear systems it can be shown that the 'normalized' frequency interval $(\omega - \omega_0)/\omega$ (where ω is the impressed frequency and ω_0 is the frequency of self-excitation) within which one observes entrainment, is proportional to h/h_0, where h is the amplitude of the impressed motion and h_0 is the amplitude of the self-excited oscillation. In case of entrainment one would expect to find a common phase difference between the motion of adjacent blades which implies also motion with a common flutter frequency. This latter phenomenon is also termed stalling flutter, although the term limit-cycle vibration is sometimes used to emphasize the constant-amplitude nature of the motion, which is often in the fundamental torsional mode.

Finally it should be noted that the distinction between blade instability (flutter) and flow instability (rotating stall) is not always perfectly distinct. When the sporadic stall flutter occurs it is clear that there is no steady tangentially propagating feature of the instability. Similarly, when propagating stall occurs with little or no vibration (stiff blades away from resonance) it is apparent that the instability is not associated with vibratory motion of the blade. However, the limit cycle type of behavior can be looked upon (due to the simultaneously observed constant interblade phase relationship) as the propagation of a disturbance along the cascade. Furthermore, the vorticity shed downstream of the blade row would have every aspect of a propagation stall region. For instance if the interblade phasing was 180 degrees the apparent stall region would be on one blade pitch in tangential extent and each would be separated by one blade pitch of unstall ed throughflow. The tangential wavelength is two blade pitches. Because of the large number of such regions, and the small tangential extent of each, this situation is still properly termed stall flutter since the blades are controlling and the blade amplitudes are constant. At the other extreme when one or two stall patches appear in the annulus it is obvious that the flow instability is controlling and then the phase relationships between adjacent blade's motions may appear to be rather sporadic. At any rate, in the middle ground between these extremes it is probable that a strong interaction between flow stability and blade stability exists and the two phenomena cannot be easily separated.

Another distinction may be attempted to assist in understanding the operative phenomena. When a *single airfoil* is subjected to an increasing angle of attack an instability of the fluid may arise, related to the Karman vortex frequency or the extension of this concept to a distributed frequency spectrum. If the frequency of this fluid instability coincides with the natural frequency of the blade in any mode the phenomenon is termed buffeting. If the dynamic moment coefficient (or force coefficient) attains a negative slope a self-excited vibration known as stall flutter occurs. The two phenomena may merge when airfoil vibration exerts some influence on the vortex shedding frequency. Stall -flutter is usually observed in the torsional mode and buffeting in the bending mode, but this distinction is not always possible. These concepts cannot be carried over directly to the cascade where steady bending amplitudes of the limit cycle variety have been observed. The explanation rests on the additional degrees of freedom present in the cascaded configuration.

7 Stall Flutter in Turbomachines

On account of the foregoing complications and the very recent emergence of quantitative CFD-based theories noted in chapter "Stall Flutter" it is not surprising that past prediction for turbomachines has rested almost entirely on correlation of experimental data. The single most important parameter governing stall ing is the incidence, and the reduced frequency has been seen in all aeroelastic formulations to exert a profound influence. Hence it is not surprising that these variables have been used to correlate the data.

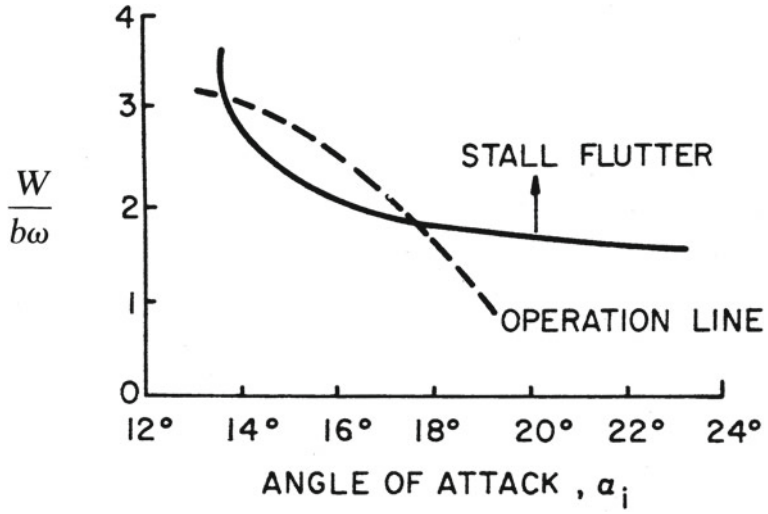

Fig. 9 Experimental stall flutter correlation

Typically stall flutter will occur at part-speed operation and will be confined to those rotor stages operating at higher than average incidence. With luck the region of flutter will be above the operating line on a compressor map and extend up to the surge line. Under less fortunate circumstances the operating line will penetrate the flutter region. The flutter boundary will have the appearance shown on Fig. 9. Contours of constant flutter (or limit cycle oscillation) stress (or tip amplitude) will run more or less parallel to, and within, the boundary. Traditional parameters for this typical experimental correlation are reduced velocity, $W/b\omega$, (the inverse of reduced frequency) and incidence, at some characteristic radius such as 75% or 80% of the blade span for a cantilever blade. The curve is typical of data obtained in turbomachines or cascades; essentially a new correlation is required for each major change of any aerodynamic variable (Mach number, stagger, blade contour, etc.). The structural mode shape will usually be first torsion. The single contour shown in the previous figure is for that level of cyclic stress (or strain) in the blade material that is arbitrarily taken to represent some distinct and repeatable measurement attributable to the flutter vibration and discernible above the 'noise' in the strain measuring system. A typical number might be a stress of 10,000 kPa used to define the flutter boundary. However, small changes in relative airspeed, W, may increase the flutter stress substantially, or, in the case of 'hard' flutter, a small increase in incidence might have a similar effect. Hence, in keeping with the nonlinear behavior described in chapter "Stall Flutter", the contours of constant flutter stress may be quite closely spaced in some regions of the correlation diagram.

Naturally, when considering three-dimensional effects it is the net energy passing from airstream to airfoil that determines whether flutter will occur, or not. The stall ed tip of a rotor blade, for example, must extract more energy from the airstream than

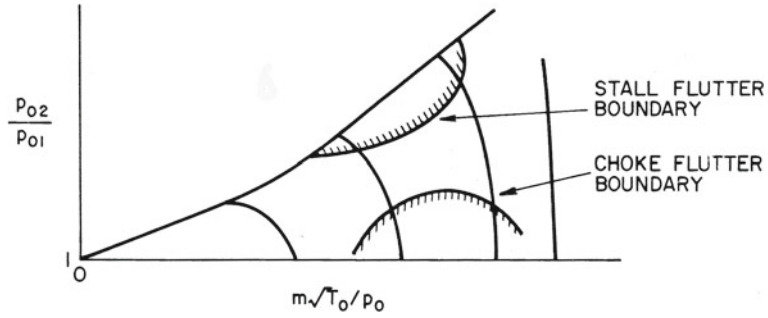

Fig. 10 Stall flutter boundary

is put back into the airstream by airfoil sections at smaller radii and that is dissipated from the system by damping.

This total description of stall flutter in turbomachine rotor blades is consistent with the appearance of the stall flutter boundary as it appears on the following typical compressor performance map (Fig. 10), the vibrations are usually confined to the first two or three stages. This figure may be viewed in conjunction with the performance map on Fig. 4 which shows typical angles of attack for a rotor blade tip in the first stage of a compressor. Keeping in mind that the mass flow parameter $\dot{m}\sqrt{T_0/p_0}$ is virtually proportional to the throughflow velocity in the first few stages of a compressor, it is clear that any typical operating line as shown on the compressor map will traverse the flutter boundary somewhat as the dotted line on Fig. 9.

This explains the general shape and location of the region of occurrence of stall flutter. Experimental determinations confirm increasing stresses as the region is penetrated from below and the specific behavior is a function of the aeroelastic properties of the individual machine, consistent with the broad principles enunciated here.

8 Choking Flutter

In the middle stages of a multistage compressor it may be possible to discern another region on the compressor map wherein so-called choking flutter will appear. This will normally occur at part-speed operation and will be confined to those rotor stages operating at lower than average incidence (probably negative values are encountered). The region of flutter will normally lie below the usual operating line on a compressor map, but individual stages may encounter this type of instability without greatly affecting operating line; this is particularly true when the design setting angle of a particular row of rotor blades has been arbitrarily changed from the average of adjacent stages through inadvertence or by a sequence of aerodynamic redesigns.

The physical manifestation of choking flutter is usually discriminated by a plot of a stage's operating line on coordinates of relative Mach number vs. incidence, as

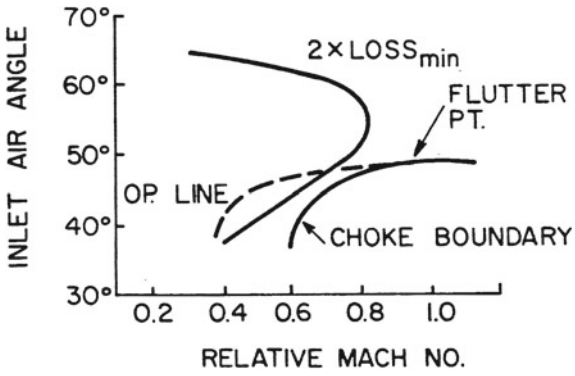

Fig. 11 Choking flutter correlation

in Fig. 11. On these same coordinates the choke boundaries are shown; a coincidence or intersection of these graphs indicate the possible presence of choking flutter and is usually confined to a very small range of incidence values. The mechanism of choking flutter is not fully understood. It is related to compressibility phenomena in the fluid and separation of the flow is probably also involved. The graph labelled '$2 \times Loss'_{min}$ is a locus of constant aerothermodynamic loss coefficient (closely related to the drag coefficient of an airfoil); the interior of the nose-shaped region representing low values of loss, or efficient operation of the compressor stage. The curve labelled 'choke boundary' represents the combination of relative Mach number and flow angle at which the minimum flow area between adjacent blades (the throat) is passing the flow with the local sonic velocity. Presumably separation of the flow at the nose of each airfoil on the pressure surface, and the *relative* motion between adjacent blades as they vibrate, conspire to change the effective throat location in a time dependent manner. These oscillatory changes effect the pressure distribution on each blade in such a fashion (including a phase angle) as to pump energy from the airstream into the vibration and thus sustain the presumed motion.

Experimental results [13, 14] bear out the general description of choking flutter described above. The analytically-based predictions [15, 16] lend further credence to the mechanism, although the aerodynamic formulation is confined to quasisteady time dependence. Ultimately a satisfactory explanation and prediction technique will be likely attained with a time marching computational capability using the compressible Navier-Stokes equations.

Choking flutter occurs in practice with sufficient frequency and destructive potential as to be an important area for current research efforts as noted above.

9 Aeroelastic Eigenvalues

Traditionally the analytical prediction of flutter has been conducted by computation of the aeroelastic eigenvalues for the particular system under investigation. In turbomachines the eigenvalue determinations have been conducted in the frequency

domain, and the unsteady aerodynamics, excluding separated or choked flow, have been based on the solutions of the small disturbance equations as described in [3–6] and elsewhere, and as reviewed effectively in the AGARD Manual [1]. A representative sample analysis for the steady loading effect in an infinite cascade was introduced in Sect. 4. In the literature a large number of additional effects are treated, including compressibility, finite flow deflection, three-dimensionality, finite shock strength and shock movement, section thickness and turbine-type geometry.

In every case, however, the initial formulation of the eigenvalue problem for an N-bladed annular cascade results in a system of mN equations, where m is the number of degrees of freedom (or else structural modes) assigned to each blade. Since the disc on which the turbomachine blades are attached will not be completely rigid, these modeshapes will be 'system' modes in which nodal circles and diameters may be discerned on the disc proper (and its extension into the flow annulus).

$$-\omega^2[M_n]\{q_n\} + [M_n\omega_n^2(1 + ig_n)]\{q_n\} = \pi b^3\omega^2[F]\{q_n\} \tag{9.1}$$

In (9.1) the aeroelastic equation has been specialized for one degree of freedom per blade ($m = 1$); hence n ranges from 0 to N-1. This equation, adapted from Crawley's Chap. 19 in [2], assumes harmonic time dependence at frequency ω and the nth blade has its individual mass, M_n, natural frequency, ω_n, and the structural damping coefficient, g_n. The development leading to (9.1) parallels that for (3.7.32) for a single foil. (The principal result of considering $m > 1$ is to replace each matrix element by a submatrix and enlarge the displacement vector, $\{q_n\}$).

When the blades on the disc are structurally uncoupled (rigid disc and no interconnecting shrouds or lacing wires) the square matrices on the LHS are diagonal and the equations are coupled only through the aerodynamic force matrix

$$[F] = \begin{bmatrix} F_0 & F_{N-1} & F_{N-2} & \dots & F_1 \\ F_1 & F_0 & F_{N-1} & \dots & F_2 \\ \cdot & \cdot & \cdot & & \cdot \\ \cdot & \cdot & \cdot & & \cdot \\ F_{N-1} & F_{N-2} & F_{N-3} & \dots & F_0 \end{bmatrix} \tag{9.2}$$

The matrix is completely populated and each element is an aerodynamic influencecoefficient: the force effect on the row-identified blade due to the motion of the column-identified blade. These are the terms derivable from the previously described analytical theories under the assumption of constant interblade phase angle, σ, and harmonic displacement given by

$$q_n = Re[\bar{q}_n \exp(i\omega t)] \tag{9.3}$$

although Fourier decomposition of the aerodynamic force is necessary to obtain the form implied by (9.1) and (9.2).

For a 'tuned' stage the mass, natural frequency and damping coefficient for every blade are the same so that the N equations are identical ($[F]$ is circulant) and the

complex eigenvalues

$$\omega = \omega_R + i\omega_I \tag{9.4}$$

may be obtained from any one of the individual blade equations. Since there are N possible tuned values of σ, there are N possible $[F]$ matrices and N corresponding eigenvalues. The particular eigenvalue that obtains in practice will be for those values of airspeed W (embedded in F) and g_n that just produce $\omega_I = 0$. That is, the typical V, g plot is replaced by a family of contours with σ as the parameter. The critical flutter speed is then obtained by minimizing W with respect to σ, see [10]. In this sense the aeroelastic behavior of tuned cascades is a straightforward extension of the single airfoil procedure, to include an additional parameter, the interblade phase angle.

One of the most intensive recent efforts in turbomachine aeroelastic studies has been in the area of 'mistuned' blade rows. When the mass and/or stiffness of all airfoils are not identical, or the coupling through the discs or shrouds is not uniform, then structural mistuning is present. Analogous aerodynamic mistuning results from nonuniform blade spacing, setting angle of section profile. Such mistuned stages are inevitably manufactured, subject in degree to inspection and tolerance acceptance procedures at assembly. The general effect of mistuning is to reduce the symmetry and cyclical nature of the matrices in the flutter equation, (8.9.1). The character of the eigenvalue plots and the eigenfunctions become more varied. Thus, at flutter, all blades are found to vibrate with the same frequency; the relative blade amplitudes and phase angles are constant with respect to time, but not with respect to location in the blade row. For each of the eigensolutions, however, there may be associated a 'tuned' interblade phase angle [2]. The most significant effect of mistuning is to change the value of ω_I. If the shift of the least stable eigenvalue is in the direction of increased stability, the proclivity to flutter is reduced and it is for this reason that mistuning is considered to be a powerful design tool for improving aeroelastic stability in cascaded airfoils. Figures 12a and 12b adapted from [11] show the effect of mistuning on the position of the eigenvalues (actually $i\omega$ rather than ω) for a 14-blade cascade.

It is demonstrated that a necessary but not sufficient condition for aeroelastic stability is that the blades be self-damped; the effect of a blade's motion upon itself must be to contribute positive aerodynamic damping. The unsteady interactions amongst or between blades in the cascade are destabilizing for at least one possible σ. This blade-to-blade destabilizing interference is reduced by mistuning and is hence desirable. Mistuning, however, can never produce stability when self-damping is negative. With nonzero structural damping, blades of larger (blade to air) mass ratio are relatively more stable.

The effect of kinematic coupling (e.g. the presence of some bending displacements in a predominantly torsional mode) may be quite important in determining stability whereas dynamic coupling (e.g. through the aerodynamic reactions) is usually not strong enough to be of significance. The effect of mean loading is speculated as being a possible source of flutter near stall, and stability trends with reduced velocity are

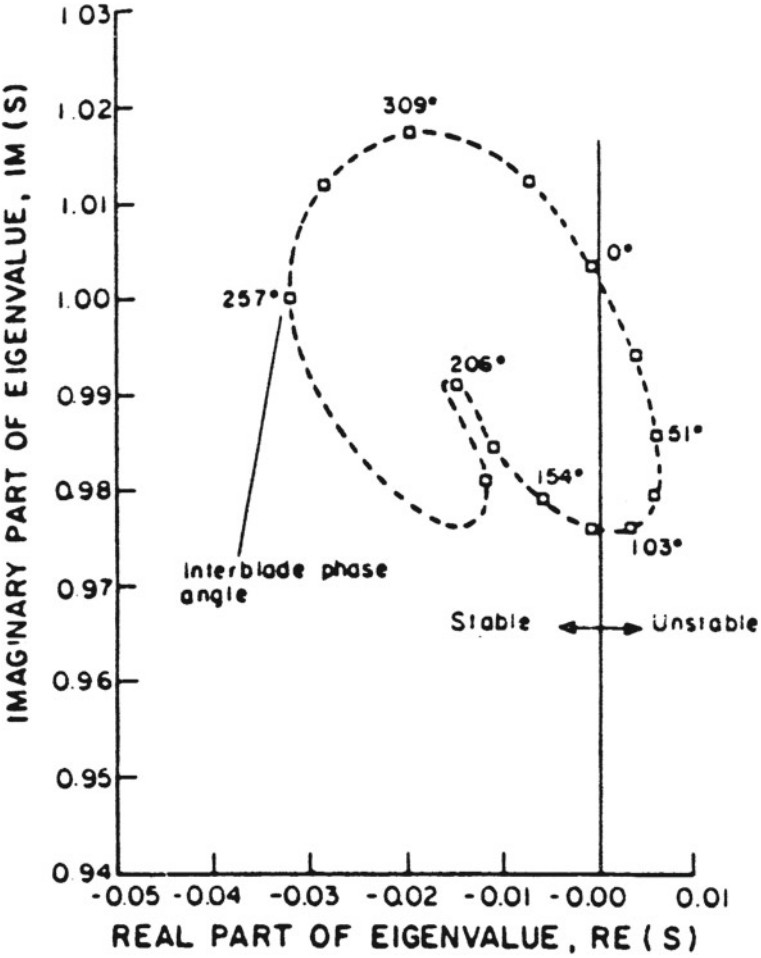

Fig. 12 **a** Aeroelastic eigenvalues of a 14-bladed tuned rotor. **b** Eigenvalues of the same rotor with 'optimal' mistuning

discussed qualitatively in [2], noting both structural and aerodynamic implications of the reduced frequency parameter.

Optimal mistuning as an intentional manufacturing procedure at assembly is an important concept, although it must be tempered with the knowledge that, under forced aerodynamic resonance, so-called 'rogue' blades may be identified which will vibrate at dangerously high amplitude. More research on mistuning may be expected to yield increasingly practical results for the turbomachine aeroelastician to apply beneficially, see [17–19].

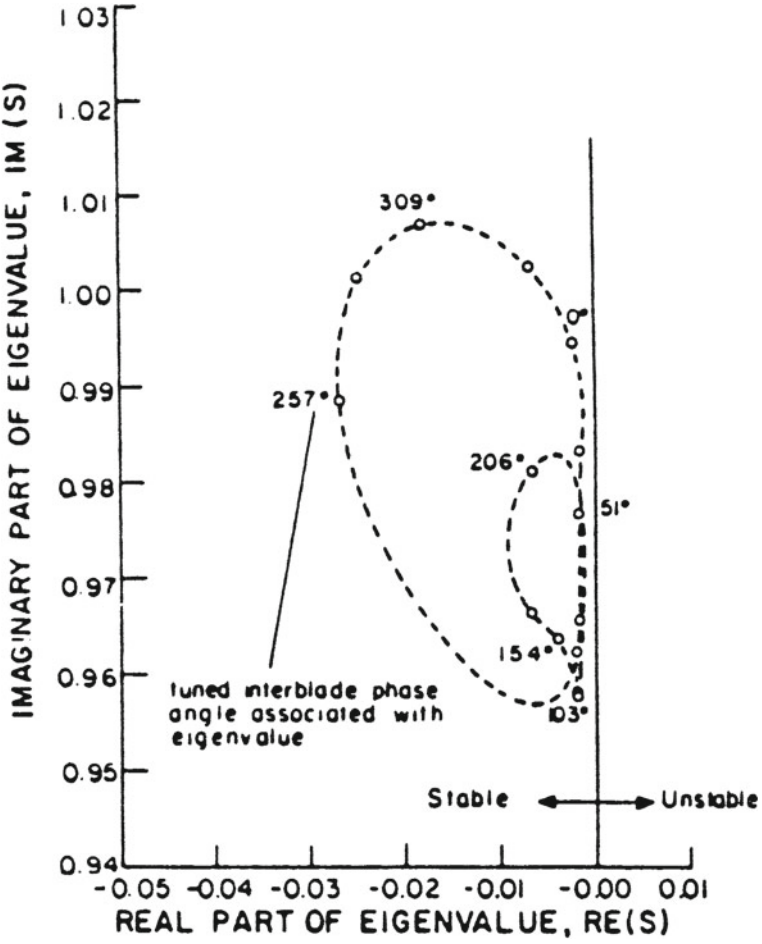

Fig. 12 (continued)

10 Recent Trends

A number of supersonic flutter regimes have been encountered in practice, see Regions III, IV and V in Fig. 13. Only Region III flutter, in either pitching or plunging, will usually be encountered along a normal operating line, and then only at corrected overspeed conditions. Supersonic aerodynamic theories have been developed to explain and confirm Region III flutter. Low incidence formulations were reported by a number of investigators, with greatest interest being attached to the onset flows having a subsonic axial component. The survey papers by Platzer [21–24] give an excellent summary of the early aerodynamics literature and experience

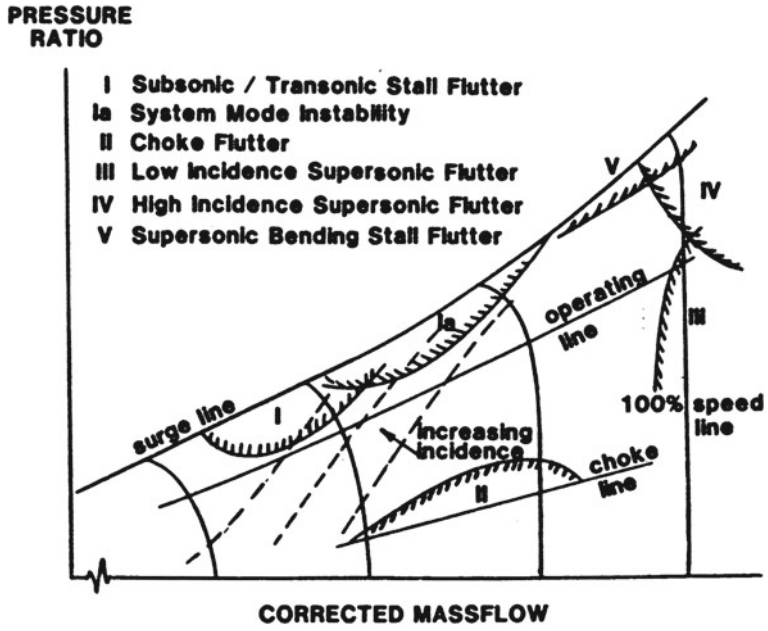

Fig. 13 Axil compressor or fan characteristic map showing principle types of flutter and region of occurrence

up to 1982 including summaries of relevant papers by authors in the former Soviet Union.

Regions IV and V in Fig. 13 are at higher compressor pressure ratio, above the normal equilibrium operating line, and, in Region V, may involve stall ing at supersonic blade relative Mach number. Unsteady aerodynamic analyses appropriate to this regime have been presented [25, 26]. For the first time account was taken of the effect of shock waves which may appear when the surface Mach number exceeds unity. Flutter observed in these regions have been mostly flexural, although not exclusively. In Region V stall ing of the flow has been implicated since the region is in the neighborhood of the surge or stall limit line. Hence Region V is provisionally termed 'supersonic bending stall flutter' and it is assumed that there is a detached bow shock at each blade passage entrance; i.e., the passage is unstarted. By contrast, the flutter mechanism in Region IV is thought to involve an in-passage shock wave whose oscillatory movement is essential for the instability mechanism.

A counterclockwise continuation around Fig. 13 returns one to Region I, divided earlier in Fig. 10 and which, it now appears, should be divided into more than one subregion. The so-called system mode instability seems to be associated with the upper end of this region, and although the blade loading is high, flutter may not involve flow separation as an essential part of the mechanism. Instead it has been hypothesized [27] that even with a subsonic onset flow the surface Mach number can exceed unity locally and oscillating shocks may help explain the appearance

of negative aerodynamic damping. It seems that these instability mechanisms (separation, oscillating shocks) may both appear in this general region of the fan or compressor map, although not both at the same time in a particular machine. Thus the non-aerodynamic factors, which are not revealed by the map parameters and are discussed in Sect. 1, may determine which, if any, of these flutter types will manifest itself in any particular instance. The clarification of this matter is still required so that Region I is now provisionally labelled Subsonic/Transonic Stall Flutter and System Mode Instability. Region II, discussed in Sect. 8 and of relatively lesser importance, is associated with choking of the passage and is labelled Choke Flutter. As such the role of oscillatory shock waves is again indicated to be important. Hence for relatively low negative incidence and high enough subsonic relative Mach numbers, appropriate to a middle stage of a multistage compressor, the mechanism of choke flutter has many similarities to the transonic stall flutter of Region I. In addition, some authors [28] add a second sub-region at a larger negative incidence and lower relative Mach number, and term it negative incidence stall flutter. The choke flutter mechanism is still controversial; it may involve the type of machine (fan, compressor or turbine), type of stage (front, middle, or rear) and structural details (shrouded vs unshrouded, disc vs drum, etc.).

Three-dimensional unsteady cascade flow was first formulated in the 1970s [29, 30]. In order to apply two-dimensional theory to the aeroelastic problems of real blade systems one must either use a representative section analysis or else apply the strip hypothesis; i.e., the aerodynamics at one radius is uncoupled from the aerodynamics at any other radius. In particular, it is known that at 'aerodynamic resonance' the strip theory breaks down and the acoustic modes are strongly coupled radially.

Along with aerodynamic advances the structural description of the blade d-disc assembly [31, 32], has received a great impetus, and the importance of forward and backward travelling waves has been firmly established. Within a particular number of nodal diameters, coupling between modes has been shown to be significant [33] and the role of the 'twin modes' (i.e. $\sin n\phi$ and $\cos n\phi$) in determining propagation has been clarified. Ford and Foord [34] have used the twin mode concept in both analysis and flutter measurement. Furthermore, the number of nodal diameters affects the fundamental natural frequencies slightly so that they cluster together. Coupling of modes with closely spaced frequencies by aerodynamic means therefore becomes appreciable and the resulting flutter mode may contain significant content from two or three modes with consecutive numbers of diametral nodes.

A great concentration of studies recently has been in the area of Computational Fluid Dynamics (CFD) coupled with a Finite Element Method (FEM) description of the blade and disk structure. Typically these sets of governing equations are solved interactively in a time marching fashion to yield the developing flutter amplitudes. Stability limits are not determined directly per se. For nonlinear systems the limit cycle amplitudes are predicted while for linear systems the temporal growth of amplitude identifies those values of the operating variables that lie within the instability boundary.

Usually in these models only spanwise displacements in plunging, pitching and surging are allowed, leading to beam -type finite elements for representing a tapered,

twisted blade of variable cross-section [35, 36]. Consequently, when plate- or shell-type elements are necessitated by airfoil thicknesses on the order of 4 or 5%, the chordwise deformations cannot be neglected and full three-dimensional FEM packages must be utilized. Essentially the camber schedule of the blade profiles change with time in these cases.

The FEM-based structural analysis is also essential for static aeroelastic studies in the nascent field of compliant blade performance modification. The compliance of the blade in an annular cascade represents a *passive* means of controlling the aerothermodynamic performance of the turbomachine by aeroelastic tailoring. This topic comes under the overarching subject of aeroservoelasticity, the application of automatic control theory to fundamental aeroelastic problems. In the blading of turbomachinery the enhanced compliance, and its chordwise distribution, are introduced intentionally by design. The resulting configuration must be checked for freedom from dynamic aeroelastic instability, or flutter, over the entire operating range of the compressor map such as that appearing in Fig. 4. It may be remarked that the concept of performance "map" will have to be extended to include the parametric ependence of performance on a representative value of a new dimensionless quantity: the ratio of the dynamic pressure of the fluid to the Young's modulus of the structure. In effect the augmentation of compliance introduces variable geometry into the turbomachine blading.

The small compliance, or conversely great rigidity, of conventional blades is responsible for only slight amounts of untwist and uncambering. In the design and development of traditional turbomachines these effects, in turn, have been reflected in very slight corrections to the aerothermodynamic performance as compared to assuming complete rigidity of the airfoils. This situation will be changed with the application of static aeroservoelasticity to the design of turbomachines with compliant blades.

Applications of unsteady Navier-Stokes codes to cascaded airfoils appear in references [37][38] and [39]. These early studies using Navier-Stokes solvers for unsteady flows with moving boundaries are chiefly of interest for computational prediction. At present the needed confidence and accuracy are not being obtained because of the inadequacy of the turbulence model in the CFD code and the extreme requirements on computer capacity alluded to above.

Subjects receiving attention recently that have not been treated fully include such topics as finite shock motion, variable shock strength, thick and highly cambered blades in a compressible flow, and the effects of curvilinear wakes and vorticity transport. These and other large amplitude and therefore nonlinear perturbations, which prevent the linear super-position implicit in classical modal analysis, have certain implications relative to the traditional solutions of the aeroelastic eigenvalue problem. The field of aeroelasticity in turbomachines continues to be under active investigation, driven by the needs of aircraft powerplant, gas turbine and steam turbine designers.

References

1. Platzer MF, Carta FO (eds) (1987) AGARD manual on aeroelasticity in axial-flow turbomachines, unsteady aerodynamics vol 1, AGARDograph No.298
2. Platzer MF, Carta FO (eds) (1988) Ibid vol 2, structural dynamics and aeroelasticity, AGARDograph No. 298
3. Whitehead DS (1960) Force and moment coefficients for vibrating aerofoils in cascade, ARC R & M 3254. London
4. Smith SM (1972) Discrete frequency sound generation in axial flow turbomachines, ARC Ri & M 3709. London
5. Verdon JM, Caspar JR (1984) A linearized unsteady aerodynamic analysis for transonic cascades. J Fluid Mech 149:403–429
6. Adamczyk JJ, Goldstein ME (1978) Unsteady flow in a supersonic cascade with subsonic leading edge locus. AIAA J 16(12):1248–1254
7. Goldstein ME (1976) Aeroacoustics. McGraw-Hill Publishing Company, New York
8. Speziale CG, Sisto F, Jonnavithula S (1986) Vortex simulation of propagating stall in a linear cascade of airfoils. ASME J Fluids Eng 108(3):304–312
9. Sisto F, Wu W, Thangam S, Jonnavithula S (1989) Computational aerodynamics of oscillating cascades with the evolution of stall. AIAA J 27(4):462–471
10. Tanida Y, Saito Y (1977) On choking flutter. J Fluid Mech 82:179–191
11. Jutras RR, Stall one MJ, Bankhead HR, (1980) Experimental investigation of flutter in midstage compressor designs. AIAA Paper 80–0786:729–740
12. Micklow J, Jeffers J (1981) Semi-Actuator disc theory for compressor choke flutter, NASA Contractor Report 3426
13. Tang ZM, Zhou S (1983) Numerical prediction of choking flutter of axial compressor blades. AIAA Paper 83–0006, Reno
14. Lane F (1956) System mode shapes in the flutter of compressor blade rows. J Aeronaut Sci 23(1):54–66
15. Crawley EF, Hall KC (1985) Optimization and mechanism of mistuning in cascades. J Eng Gas Turbines Power 107(2):418–426
16. Bendiksen OO, Valero NA (1987) Localization of natural modes of vibration in bladed disks. ASME Paper 87-GT-47, Anaheim, California
17. Kaza KR, Kielb RE (1982) Flutter and response of a mistuned cascade in incompressible flow. AIAA J 20(8):1120–1127
18. Srinavasan AV (1980) Influence of mistuning on blade torsional flutter, NASA CR-165137
19. Platzer MF (1975) Transonic blade flutter: a survey. Shock Vib Dig 7(7):97–106
20. Platzer MF (1977) Unsteady flows in turbomachines-a review of current developments. In: AGARD-CP-227 unsteady aerodynamics, Ottawa
21. Platzer MF (1978) Transonic blade flutter: a survey of new developments. Shock Vib Dig 10(9):11–20
22. Platzer MF (1982) Transonic blade flutter: a survey of new developments. Shock Vib Dig 14(7):3–8
23. Adamczyk JJ (1978) Analysis of supersonic stall bending flutter in axial-flow compressor by actuator disc theory. NASA, Technical Paper, p 1345
24. Adamczyk JJ, Stevens W, Jutras R (1982) Supersonic stall flutter of high-speed fans. Trans ASME J Eng Power 104(3):675–682
25. Stargardter H (1979) Subsonic/Transonic stall flutter study, Final Report, NASA CR-165256, PWA 5517–31
26. Fleeter S (1979) Aeroelasticity research for turbomachine applications. J Aircr 16(5):320–326
27. Namba M (1972) Lifting surface theory for a rotating subsonic or transonic blade row, Aeronautical Research Council, R & M 3740. London
28. Salaun P (1974) Pressions aerodynamiques instationnaires sur une grille annulaire en eccoulement subsonique, Publication ONERA No. 158

29. Ewins DJ (1973) Vibration characteristics of bladed disc assemblies. J Mech Eng Sci 15(3):165–186
30. Srinivasan AV (ed) (1976) Structural Dynamic Aspects of Bladed Disk Assemblies. In: Proceedings ASME Winter Annual Meeting, New York
31. Chi RM, Srinicasan AV (1984) Some recent advances in the understanding and prediction of turbomachine subsonic stall flutter, ASME Paper 84-GT-151
32. Ford RAJ, Foord CA (1979) An analysis of aeroengine an flutter using twin orthogonal vibration modes, ASME Paper 79-GT-126
33. Sisto F, Chang AT (1984) A finite element for vibration analysis of twisted blades based on beam theory. AIAA J 22(11):1646–1651
34. Sisto F, Chang AT (1985) Influence of rotation and pretwist on cantilever fan blade flutter, In: Proceedings of 7th international symposium on airbreathing engines, Beijing
35. Rai MM (1987) Navier-Stokes simulations of rotor-stator interaction using patched and overlaid grids. AIAA J Propul Power 3(9):387–396
36. Schroeder LM, Fleeter S (1988) Viscous aerodynamic analysis of an oscillating flat plate airfoil with locally analytic solution. AIAA Paper 88–0130, Jan 1988
37. Clarkson JD, Ekaterinaris JA, Platzer MF (1991) Computational investigation of airfoil stall flutter. In: Sixth international symposium on unsteady aerodynamics and aeroacoustics and aeroelasticity of turbomachines and propeller, Notre Dame, Sept 1991